

## Time-Resolved Double Ionization with Few Cycle Laser Pulses

F. Légaré,<sup>1,2</sup> I. V. Litvinyuk,<sup>1</sup> P. W. Dooley,<sup>1,3</sup> F. Quéré,<sup>1</sup> A. D. Bandrauk,<sup>2</sup> D. M. Villeneuve,<sup>1</sup> and P. B. Corkum<sup>1</sup>

<sup>1</sup>National Research Council of Canada, Ottawa, Ontario, Canada K1A 0R6

<sup>2</sup>Département de Chimie, Université de Sherbrooke, Sherbrooke, Québec, Canada

<sup>3</sup>Department of Physics & Astronomy, McMaster University, Hamilton, Ontario, Canada

(Received 24 January 2003; published 29 August 2003)

Ionization of  $D_2$  launches a vibrational wave packet on the ground state of  $D_2^+$ . Removal of the second electron places a pair of  $D^+$  ions onto a Coulombic potential. Measuring the  $D^+$  kinetic energy determines the time delay between the first and the second ionization. Caught between a falling ionization and a rapidly rising intensity, the typical lifetime of the  $D_2^+$  intermediate is less than 5 fs when an intense 8.6 fs laser pulse is used. We simulate Coulomb explosion imaging of the ground state wave function of  $D_2$  by a 4 fs optical pulse and compare with our experimental observations.

DOI: 10.1103/PhysRevLett.91.093002

PACS numbers: 33.80.Rv, 34.50.Gb, 42.50.Hz

Femtosecond pump-probe spectroscopy is an extremely powerful technique for studying molecular dynamics [1]. However, inferring the mechanisms responsible for the dynamics from these measurements is difficult. Imaging molecular structure would be much more direct and intuitive. We show that laser induced Coulomb explosion for direct imaging of molecular structure is within reach.

Accurate Coulomb explosion imaging of molecular structure requires that the molecule reach a sufficiently high charge state for the interionic potential to be approximated by Coulomb's law [2]. This charge state must be reached while the ions are inertially confined in their original configuration. Inertial confinement is readily achieved for small molecular ions moving at megavolt kinetic energies when they pass through a thin foil [3]. However, this technique is not well suited as a probe in pump-probe measurements.

For optically driven Coulomb explosion imaging, inertial confinement has been a demanding requirement that has been satisfied only with  $\sim 50$  fs pulses in experiments involving iodine [4]. In other systems, dynamics of intermediate ionic states distorts the image [5–9]. Few cycle laser pulses [10] are now generated in a few laboratories. Such pulses should be short enough for distortion-free Coulomb explosion imaging.

Using nuclear motion (a “molecular clock” [11]) to time resolve the sequential double ionization of  $D_2$  molecules, we show that  $\sim 9$  fs optical pulses can be used to inertially confine virtually any molecule or molecular ion during its ionization phase. Both calculations and experiments with 9 fs pulses show that the two electron removal  $D_2 \rightarrow D_2^{++}$  can be performed within  $\sim 5$  fs. Furthermore, we present a simulation of Coulomb explosion imaging of  $D_2$  using currently available  $\sim 4$  fs,  $\sim 5 \times 10^{15}$  W/cm<sup>2</sup> pulses [10].

Also of interest is the fact that we achieve an ionization rate of  $\sim 10^{16}$  s<sup>-1</sup>. The very high ionization rate is due to the rapid increase in pulse intensity combined with a rapidly decreasing ionization potential due to nuclear motion. We make the transition from no ionization to

complete ionization in less than two optical cycles. Therefore, we can suppress (or control) processes that occur at larger internuclear separations even for a light molecule such as  $D_2$ .

To generate our  $\sim 9$  femtosecond pulses, the output of a Ti:sapphire regenerative amplifier (810 nm, 40 fs, 250  $\mu$ J, 500 Hz repetition rate) amplifier was coupled into a hollow core fiber (250  $\mu$ m diameter, 100 cm long) filled with 1 atm of argon. The self-phase modulation [10] during propagation of the optical pulses through the hollow fiber broadens the spectral bandwidth from 30 to 200 nm. The pulse was compressed using multiple reflections from a pair of chirped mirrors. The resulting pulses were characterized using spectral phase interferometry for direct electric-field reconstruction [12]. As shown in the inset of Fig. 1, we obtained 8.6 fs linearly polarized pulses. The main peak contains 84% of the

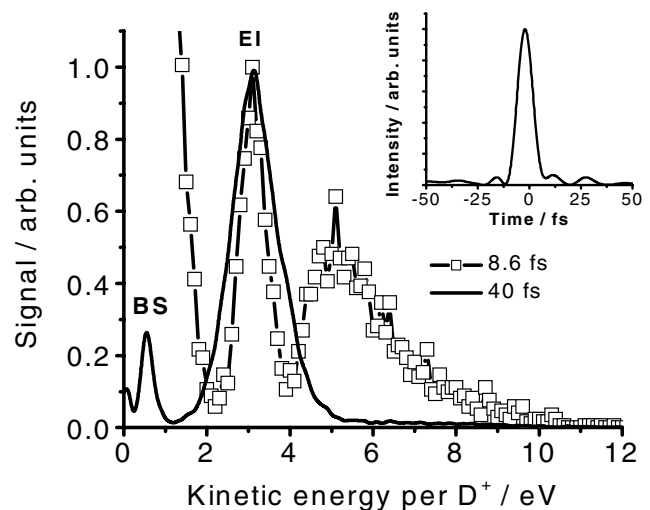


FIG. 1. Deuteron kinetic energy spectra at an intensity of  $5 \times 10^{14}$  W/cm<sup>2</sup> for linearly polarized pulse at durations of 40 fs (solid line) and 8.6 fs (squares). The time-dependent intensity profile of the 8.6 fs pulse is shown in the inset. BS: bond softening; EI: enhanced ionization.

energy and 95% is contained within a 100 fs window. An achromatic quarter wave plate was used to produce circular polarization.

The laser beam was focused inside the high vacuum experimental chamber ( $10^{-9}$  mbar background pressure) by an on-axis parabolic mirror ( $f/2$ ,  $f = 50$  mm) into a collimated beam of deuterium molecules. We estimate the beam diameter at the focus to be  $\sim 5$   $\mu\text{m}$  and the confocal parameter  $\sim 100$   $\mu\text{m}$ .

The molecular beam was produced by expanding 25 mbar of  $\text{D}_2$  through a 100  $\mu\text{m}$  aperture into the vacuum. The jet was skimmed to produce a beam with a thickness of 40  $\mu\text{m}$  (in the laser propagation direction), a height of 1.5 mm, and a density of  $\sim 10^{10}$  molecules/ $\text{cm}^3$  ( $P \approx 10^{-7}$  mbar). Since the confocal parameter of the laser beam was greater than the molecular beam's thickness, molecules see only a slight intensity variation along the laser propagation direction. The peak laser intensity was determined by measuring the recoil momentum distribution of  $\text{D}_2^+$  ions for circularly polarized pulses [13].

When a femtosecond pulse ionizes  $\text{D}_2$ , Coulomb repulsion between the deuterium ions converts their initial potential energy to kinetic energy. Coulomb explosion fragments were analyzed using an imaging time-of-flight mass spectrometer [14]. The molecular beam, mass spectrometer axis, and laser beams were mutually orthogonal. Deuterons were detected using a helical delay-line anode time- and position-sensitive detector. From the impact data, the complete velocity vector for each deuteron was determined.

The distribution of kinetic energy per deuteron is shown in Fig. 1 for linearly polarized 8.6 and 40 fs pulses. In both cases, the peak intensity is  $5 \times 10^{14}$   $\text{W}/\text{cm}^2$ . The vertical axis is normalized at 3 eV. For the 40 fs pulse, the energy spectrum is dominated by a peak around 3 eV with a smaller peak observed at  $\sim 0.7$  eV. Those features are the signature of laser field induced processes—bond softening and enhanced ionization—discussed below.

In  $\text{D}_2$  a laser pulse first creates a molecular ion. With a long ( $\geq 40$  fs) pulse the ion has enough time to undergo field-assisted dissociation [15] (known as bond softening when the field oscillates at optical frequencies [16]) before the second electron is ionized. In the process of bond softening the internuclear separation passes through a region where the ionization rate maximizes (enhanced ionization), exceeding even the rate for infinitely separated atoms by more than an order of magnitude [5,7–9]. Both processes originate in the multiphoton coupling of the  $\Sigma_g$  and  $\Sigma_u$  levels of the ion [7,8]. This coupling is efficient only for molecules parallel to the field leading to fragments that are directed primarily along the laser polarization. The peak at  $\sim 0.7$  eV in Fig. 1 comes from molecular ions that bond soften without further ionization. The peak at  $\sim 3$  eV is a signature of enhanced ionization [7,8].

An energetic fragment channel between 4–10 eV has been observed [11,17–19] with  $\sim 40$  fs pulses. Such high-

energy fragments can come only from excitation or double ionization at small internuclear separation. With 40 fs pulses, these fragments are caused by recollision [11,19] (described below). Compared with enhanced ionization, recollision is a minor dissociation channel ( $\sim 5\%$ ) and is barely observable on the linear scale in Fig. 1.

With our 8.6 fs pulse, however, 4–10 eV energy fragments represent a major dissociation channel ( $\sim 20\%$ ). By measuring the correlated spectrum we confirm that the 4–10 eV ions come from double ionization. As the pulse duration is increased from 8.6 to 40 fs, the high-energy peak shifts to lower energies until it merges into the enhanced ionization peak. We now concentrate on the physical origin of this peak.

The observed double ionization can be either sequential or nonsequential. The dominant nonsequential ionization mechanism in strong laser fields is electron recollision [11]. The first ionized electron is driven by the laser field and in linearly polarized light can inelastically scatter off its parent ion. Known as a recollision, inelastic scattering is suppressed when the ellipticity increases; i.e., the electron will miss the ion core.

Figure 2 compares results obtained with linearly ( $5 \times 10^{14}$   $\text{W}/\text{cm}^2$ ) and circularly ( $1 \times 10^{15}$   $\text{W}/\text{cm}^2$ ) polarized 10.5 fs pulses. BS and EI are present in both spectra. Both spectra also have a peak at about 5 eV that we attribute to SI. An additional feature is observed in the linear case—an energetic plateau between 6 and 10 eV (RC).

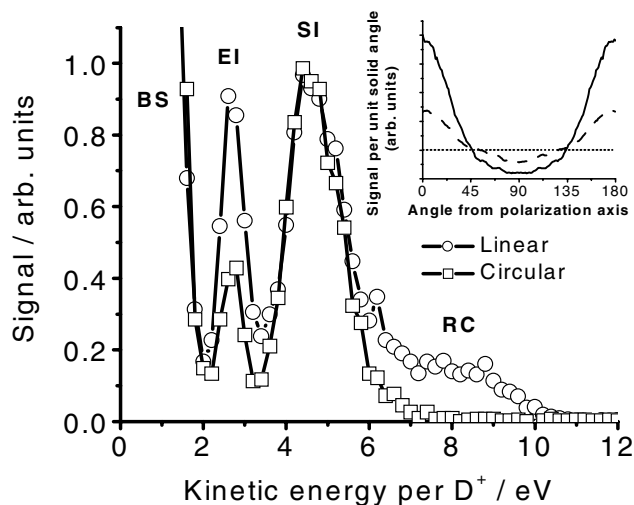


FIG. 2. Deuteron kinetic energy spectra for a 10.5 fs duration pulse with the function of polarization. The electric field amplitude is equal in both cases. The intensity in the linear case is  $5 \times 10^{14}$   $\text{W}/\text{cm}^2$ . Inset: ion signal as a function of the angle between deuteron momentum and the laser polarization axis for 0.5–4 eV deuterons (solid line), 4–10 eV deuterons (dashed line), and an isotropic distribution (dotted line). The inset data were obtained using a linearly polarized, 8.6 fs,  $2.8 \times 10^{15}$   $\text{W}/\text{cm}^2$  laser pulse. RC: electron recollision; SI: sequential double ionization.

Its polarization sensitivity shows that it is due to electron recollision. As we show below, in the other extreme of very high intensity pulses, the sequential double ionization peak grows and broadens until it dominates all other channels.

Figure 2 (inset) shows the angle dependence of the 0.5–4 eV fragments (solid line) and the 4–10 eV fragments (dashed line). Enhanced ionization and bond softening channels are more directional than sequential double ionization. While the angle-resolved data were obtained using an 8.6 fs,  $2.8 \times 10^{15}$  W/cm<sup>2</sup> pulse, the angular dependence is insensitive to the peak laser intensity or whether we include recollision in the 4–10 eV measurements.

One of our technical achievements is the use of a thin molecular beam [20]. It allows us to expose most of our target molecules to a rapidly increasing but near spatially uniform pulse intensity. Molecules experience only lower intensities in the radial extremes of the focus. Therefore, we can study sequential double ionization when the ionization rates are extremely large. The earlier the first ionization occurs, the faster the intensity will rise, and the sooner the second electron will be removed. This time difference can be measured using a molecular clock [11]. The first ionization starts the clock. The removal of the second electron promotes  $D_2^+$  to  $D_2^{++}$ , where Coulomb repulsion determines the kinetic energy of the deuterons. The deuteron kinetic energy is a measure of the time delay between first and second ionization.

Figure 3 shows the deuteron kinetic energy spectra obtained with circularly polarized light and laser intensities of  $1.2 \times 10^{15}$  W/cm<sup>2</sup> and  $2.8 \times 10^{15}$  W/cm<sup>2</sup>. At  $2.8 \times 10^{15}$  W/cm<sup>2</sup> sequential double ionization is 15 times more probable than all other channels combined. In agreement with our qualitative prediction, the kinetic

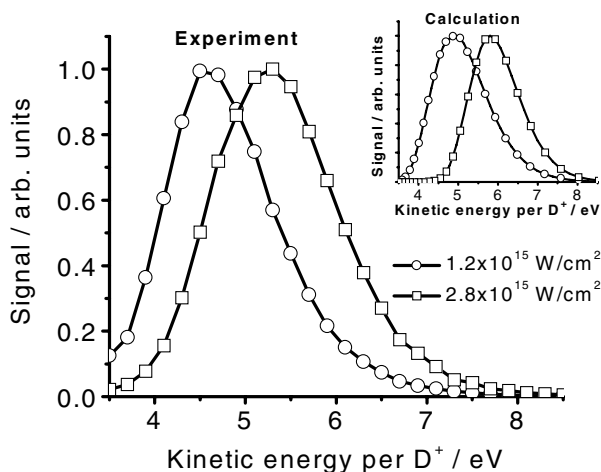


FIG. 3. Deuteron kinetic energy spectra for a 10.5 fs duration, circularly polarized pulse with an intensity of  $1.2 \times 10^{15}$  W/cm<sup>2</sup> (circles) and  $2.8 \times 10^{15}$  W/cm<sup>2</sup> (squares). Inset: calculated spectra corresponding to  $1.2 \times 10^{15}$  W/cm<sup>2</sup> (dashed line) and  $2.8 \times 10^{15}$  W/cm<sup>2</sup> (solid line).

energy of deuterons is higher at higher laser intensity. At intermediate intensities (not shown) the kinetic energies are also intermediate.

For a quantitative comparison, we now model the results for the intensities used in Fig. 3. The calculations were performed using the actual time-dependent field for the experimental pulses. We assume that the rates for both stages of the  $D_2$  ionization depend solely upon the corresponding ionization potentials and are described by atomic models [21]. The ionization potentials were calculated using potential energy surfaces for the  $D_2$  ground state and the field-coupled surface for the ground state of the  $D_2^+$ .

During the first ionization step, the ground state vibrational nuclear wave function for  $D_2$  was projected onto the  $D_2^+$  potential. The radial distortion due to the coordinate dependence of the ionization rate was taken into account [22]. The resulting wave packet was propagated on the lowest quasistatic time-dependent  $D_2^+$  potential [22] by numerical solution of the time-dependent Schrödinger equation. During the second ionization step, the wave packet was projected onto the Coulombic potential. This procedure yields the deuteron kinetic energy distribution.

In the model, we used circularly polarized light for comparison with the experimental data of Fig. 3. The total kinetic energy distribution was calculated by incoherently summing the weighted kinetic energy distributions obtained for various first and second ionization times within the duration of the pulse. The weighting factors also included the radial intensity distribution in the laser focus. The calculated kinetic energy spectra for intensities of  $2.8 \times 10^{15}$  W/cm<sup>2</sup> and  $1.2 \times 10^{15}$  W/cm<sup>2</sup> are shown in the inset of Fig. 3. In agreement with the experimental data, for higher laser intensity, the sequential double ionization peak shifts to higher energy. This is because the time delay between the first and the second ionization steps decreases.

Though in relatively good agreement with the experiment, the calculated sequential double ionization spectra overestimate the kinetic energy of the deuterons. The discrepancy corresponds to less than 1 fs in time delay. It should be noted that, while the inset of Fig. 2 shows that the ionization rate depends on the molecular orientation [13], the rate used in the model is not orientation dependent. In addition, atomic models often overestimate the molecular ionization rates [23] and the model that we used [21] does not include “over the barrier” ionization [24]. Finally, the calculation neglects the excited quasistatic state of  $D_2^+$  [22].

Figure 4 depicts the deuteron kinetic energy spectrum obtained using the most intense (8.6 fs,  $2.8 \times 10^{15}$  W/cm<sup>2</sup>) linearly polarized pulse that we can produce. For comparison, calculated kinetic energy distributions for second ionizations that occur one optical cycle (2.7 fs) and two optical cycles (5.4 fs) after the first ionization step are included in Fig. 4. The experimental

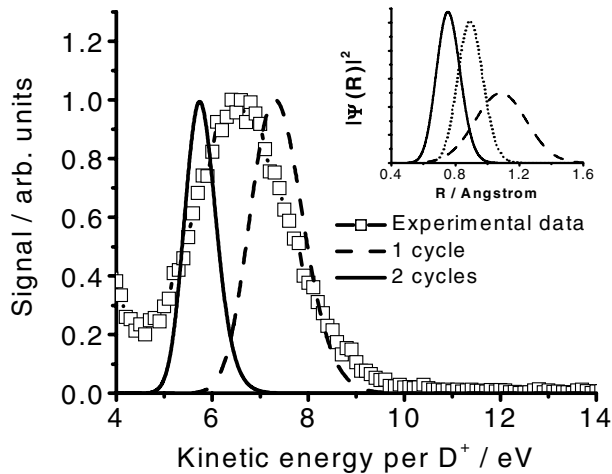


FIG. 4. Deuteron kinetic energy spectra for a linearly polarized, 8.6 fs duration pulse at intensity of  $2.8 \times 10^{15}$  W/cm<sup>2</sup> (squares). Also shown are calculated spectra for time delays of one (dashed line) and two (solid line) optical cycles between the first and second ionization steps. Inset: the density of the D<sub>2</sub> wave function for the ground state (solid line), Coulomb explosion image assuming a 4 fs pulse (dotted line), and the reconstructed image derived from the experimental spectrum of Fig. 4 (dashed line).

distribution peaks between the two calculated curves, suggesting that double ionization occurs on the average within 4 fs.

In conclusion, few cycle pulses will allow nuclear motion to be frozen for almost any molecule. The inset in Fig. 4 depicts the density of the ground state wave function of D<sub>2</sub> (solid line), the Coulomb explosion image predicted for a 4 fs,  $5.6 \times 10^{15}$  W/cm<sup>2</sup> circularly polarized pulse (dotted line), and the reconstructed image [25] obtained from the experimental deuteron spectrum of Fig. 4 (dashed line). However, the calculation reveals that  $\sim 50\%$  of the shift in the wave function's position imaged is caused by the ionization rate's dependence on the nuclear coordinate. The rest is nuclear motion. While nuclear motion will be slower in heavier molecules, the ionization rate's dependence on the nuclear coordinate will always be an important issue in Coulomb explosion imaging. To obtain accurate molecular structures, its influence will have to be removed.

Experiments with near single cycle pulse will face a new issue. For linear polarization, two electrons would need to occupy the barrier region simultaneously. This will surely impede the ionization process. By comparing linear and circular polarization, we expect to observe a Coulomb blockade in strong field ionization analogous to the Coulomb blockade studied in solid-state devices [26]. We expect that multielectron ionization with few cycle pulses will require circular polarized light.

The authors appreciate financial support from Canada's Natural Science and Engineering Research Council, Photonics Research Ontario, the Canadian Institute for Photonics Innovation, and Le Fonds Québécois de la

Recherche sur la Nature et les Technologies. We acknowledge C. Ellert for his valuable contributions to this work.

- 
- [1] A. H. Zewail, *J. Phys. Chem. A* **104**, 5660 (2000).
  - [2] Z. Vager, R. Naaman, and E. P. Kanter, *Science* **244**, 426 (1989).
  - [3] E. P. Kanter, P. J. Cooney, D. S. Gemmell, K.-O. Groeneveld, W. J. Pietsch, A. J. Ratkowski, Z. Vager, and B. J. Zabransky, *Phys. Rev. A* **20**, 834 (1979).
  - [4] D. T. Strickland, Y. Beaudoin, P. Dietrich, and P. B. Corkum, *Phys. Rev. Lett.* **68**, 2755 (1992).
  - [5] K. Codling, L. J. Frasinski, and P. A. Hatherly, *J. Phys. B* **22**, L321 (1989).
  - [6] M. Schmidt, D. Normand, and C. Cornaggia, *Phys. Rev. A* **50**, 5037 (1994).
  - [7] T. Seideman, M. Yu. Ivanov, and P. B. Corkum, *Phys. Rev. Lett.* **75**, 2819 (1995).
  - [8] T. Zuo and A. D. Bandrauk, *Phys. Rev. A* **52**, R2511 (1995).
  - [9] E. Constant, H. Stapelfeldt, and P. B. Corkum, *Phys. Rev. Lett.* **76**, 4140 (1996).
  - [10] M. Nisoli, S. De Silvestri, O. Svelto, R. Szpöcs, K. Ferencz, Ch. Spielman, S. Sartania, and F. Krausz, *Opt. Lett.* **22**, 522 (1997).
  - [11] H. Niikura, F. Légaré, R. Hasbani, A. D. Bandrauk, M. Yu. Ivanov, D. M. Villeneuve, and P. B. Corkum, *Nature (London)* **417**, 917 (2002).
  - [12] C. Iaconis and I. A. Walmsley, *Opt. Lett.* **23**, 792 (1998).
  - [13] I. V. Litvinyuk, K. F. Lee, P. W. Dooley, D. M. Rayner, D. M. Villeneuve, and P. B. Corkum, *Phys. Rev. Lett.* **90**, 233003 (2003).
  - [14] P. W. Dooley, I. V. Litvinyuk, K. F. Lee, D. M. Rayner, D. M. Villeneuve, and P. B. Corkum, *Phys. Rev. A* (to be published).
  - [15] G. R. Hanson, *J. Chem. Phys.* **62**, 1161 (1975).
  - [16] A. Zavriyev, P. H. Bucksbaum, H. G. Muller, and D. W. Schumacher, *Phys. Rev. A* **42**, R5500 (1990).
  - [17] C. Trump, H. Rottke, and W. Sandner, *Phys. Rev. A* **60**, 3924 (1999).
  - [18] A. Staudte, C. L. Cocke, M. H. Prior, A. Belkacem, C. Ray, H. W. Chong, T. E. Glover, R. W. Schoenlein, and U. Saalmann, *Phys. Rev. A* **65**, 020703(R) (2002).
  - [19] H. Sakai, J. J. Larsen, I. Wendt-Larsen, J. Olesen, P. B. Corkum, and H. Stapelfeldt, *Phys. Rev. A* **67**, 063404 (2003).
  - [20] P. W. Dooley, V. R. Bhardwaj, and P. B. Corkum, in *Proceedings of the International Conference on Lasers 1999* (STS Press, McClean, VA, 2000), p. 8.
  - [21] G. L. Yudin and M. Yu. Ivanov, *Phys. Rev. A* **64**, 013409 (2001).
  - [22] P. Dietrich, M. Yu. Ivanov, F. A. Ilkov, and P. B. Corkum, *Phys. Rev. Lett.* **77**, 4150 (1996).
  - [23] S. Hankin, D. M. Villeneuve, P. B. Corkum, and D. M. Rayner, *Phys. Rev. Lett.* **84**, 5082 (2000).
  - [24] S. Augst, D. Strickland, D. D. Meyerhofer, S. L. Chin, and J. H. Eberly, *Phys. Rev. Lett.* **63**, 2212 (1989).
  - [25] S. Chelkowski, P. B. Corkum, and A. D. Bandrauk, *Phys. Rev. Lett.* **82**, 3416 (1999).
  - [26] A. Imamoglu and Y. Yamamoto, *Phys. Rev. Lett.* **72**, 210 (1994).